Fryer, P., Pearce, J. A., Stokking, L. B., et al., 1992
*Proceedings of the Ocean Drilling Program, Scientific Results,* Vol. 125

# 33. ROCK MAGNETIC STUDIES OF SERPENTINITE SEAMOUNTS IN THE MARIANA AND IZU-BONIN REGIONS[1]

L. B. Stokking,[2] D. L. Merrill,[2] R. B. Haston,[3] J. R. Ali,[4] and K. L. Saboda[5]

## ABSTRACT

During Leg 125, scientists drilled two serpentinite seamounts: Conical Seamount in the Mariana forearc and Torishima Forearc Seamount in the Izu-Bonin forearc. Grain densities of the serpentinized peridotites range from 2.44 to 3.02 g/cm$^3$. The NRM intensity of the serpentinized peridotites ranges from 0.01 to 0.59 A/m and that of serpentine sediments ranges from 0.01 to 0.43 A/m. Volume susceptibilities of serpentinized peridotites range from $0.05 \times 10^{-3}$ SI to $9.78 \times 10^{-3}$ SI and from $0.12 \times 10^{-3}$ to $4.34 \times 10^{-3}$ SI in the sediments. Koenigsberger ratios, a measure of the relative contributions of remanent vs. induced magnetization to the magnetic anomaly, vary from 0.09 to 80.93 in the serpentinites and from 0.06 to 4.74 in the sediments. The AF demagnetization behavior of the serpentinized peridotites shows that a single component of remanence (probably a chemical remanence carried by secondary magnetite) can be isolated in many samples that have a median destructive field less than 9.5 mT. Multiple remanence components are observed in other samples. Serpentine sediments exhibit similar behavior. Comparison of the AF demagnetization of saturation isothermal remanence and NRM suggests that the serpentinized peridotites contain both single-domain and multidomain magnetite particles. The variability of the magnetic properties of serpentinized peridotites reflects the complexity of magnetization acquired during serpentinization. Serpentinized peridotites may contribute to magnetic anomalies in forearc regions.

## INTRODUCTION

During Ocean Drilling Program (ODP) Leg 125, scientists drilled two serpentinite seamounts in the Mariana and Izu-Bonin forearcs: four sites (Sites 778–781) on Conical Seamount, a cone-shaped structure, 1500 m high, located on the outer-arc high of the Mariana forearc basin (Fig. 1), and two sites on Torishima Forearc Seamount (Sites 783–784), part of a 500-km-long ridge along the inner wall of the Izu-Bonin Trench (Fig. 1). No serpentinized peridotites or serpentine sediments were recovered at Site 781 (Fryer, Pearce, Stokking, et al., 1990). Samples from Site 783 were not taken because of insufficient recovery of serpentinized peridotites (Fryer, Pearce, Stokking, et al., 1990). This investigation focuses on the magnetic properties of the serpentinized peridotites and the serpentine sediments derived from them (1) to determine magnetic mineralogy, (2) to evaluate how magnetic properties change with increasing serpentinization, and (3) to assess the potential contribution of serpentinized ultramafic rocks to the magnetic signatures of serpentinite seamounts and to magnetic anomalies in forearc regions.

The determination of the rock magnetic properties and the identification of the magnetic minerals of serpentine sediments and serpentinized ultramafic rocks from both regions can contribute to our understanding of the processes of serpentinization. The rock magnetic analyses focus on the characterization of magnetic properties of serpentinized peridotites and their change with increasing serpentinization. These properties then are compared to those of serpentine sediments derived from the serpentinized peridotites.

Secondary magnetite is produced during the serpentinization of peridotites by the alteration of primary olivine, orthopyroxene, clinopyroxene, and spinel. The degree of serpentinization should therefore be a factor in controlling the composition and abundance of the iron oxide phase present (Coleman, 1971; Luyendyk and Day, 1982). The amount and composition of magnetite in serpentinite also reflects the composition of the parent mineral: zones of higher magnetite abundance may indicate that the silicate parent was rich in iron (Luyendyk and Day, 1982); chromium-rich spinel may produce a chromium-rich magnetite with magnetic properties that differ from that of pure iron-magnetite (Shive et al., 1988). Rock magnetic techniques are useful for distinguishing primary iron oxide minerals from secondary phases produced during serpentinization and may aid in detection and identification of other magnetic minerals, such as hematite, pyrrhotite, and josephinite. The magnetic mineralogy therefore should reflect the composition of the primary peridotite and may provide constraints on the composition of the serpentinizing fluids.

Investigations of the magnetic properties and the potential contribution to magnetic anomalies have been performed on submarine basalts (Lowrie et al., 1973a, 1973b; Fox and Opdyke, 1973; Hall, 1976; Böhlke et al., 1981; Day et al., 1983; Smith, 1985), volcanic seamounts (Gromme and Vine, 1972; Merrill and Burns, 1972; Marshall, 1978; Kono, 1980; Furuta et al., 1980; Rice et al., 1980; Gee et al., 1988), and fracture-zone serpentinites recovered at Deep Sea Drilling Project Site 334 (Dunlop and Prevot, 1982) and from Hole 670A drilled during ODP Leg 109 (Hamano et al., 1990; Bina et al., 1990; Krammer, 1990). Magnetic anomalies produced by serpentinites have been observed (Griscom, 1964; Silver, 1969). Several scientists have studied the magnetic properties of serpentinites exposed on land in ophiolite complexes (Banerjee, 1980; Beske-Diehl and Banerjee, 1980; Luyendyk et al., 1982; Luyendyk and Day, 1982; Swift and Johnson, 1984). The magnetic properties of alpine-type serpentinites have been reported by Saad (1969a, 1969b), Coleman (1971), and Lienert and Wasilewski (1979); their variation with metamorphic grade was discussed by Shive et al. (1988). Because of the abundance of magnetite, serpentinite is strongly magnetic and may contribute greatly to the magnetic signature of serpentinite seamounts and to the magnetic anomalies in the Mariana and Izu-Bonin forearcs in general (Hussong and Fryer, 1981). However, little is known about the magnetic properties of serpentinized rocks in forearc environments. Thus, we have evaluated the potential contribution of serpentinized ultramafic rocks to the magnetic signa-

[1] Fryer, P., Pearce, J. A., Stokking, L. B., et al., 1992. *Proc. ODP, Sci. Results,* 125: College Station, TX (Ocean Drilling Program).

[2] Ocean Drilling Program, Texas A&M University, 1000 Discovery Drive, College Station, TX 77845-9547, U.S.A., and Department of Geophysics, Texas A&M University, College Station, TX 77843, U.S.A.

[3] Department of Geological Sciences, University of California, Santa Barbara, Santa Barbara, CA 93106 (present address: AMOCO Production Company, 501 West Lake Park Boulevard, P.O. Box 3092, Houston, TX 77253, U.S.A.).

[4] Department of Oceanography, The University, Southampton, SO9 5NH, United Kingdom.

[5] Hawaii Institute of Geophysics, 2525 Correa Road, Honolulu, HI 96822, U.S.A.

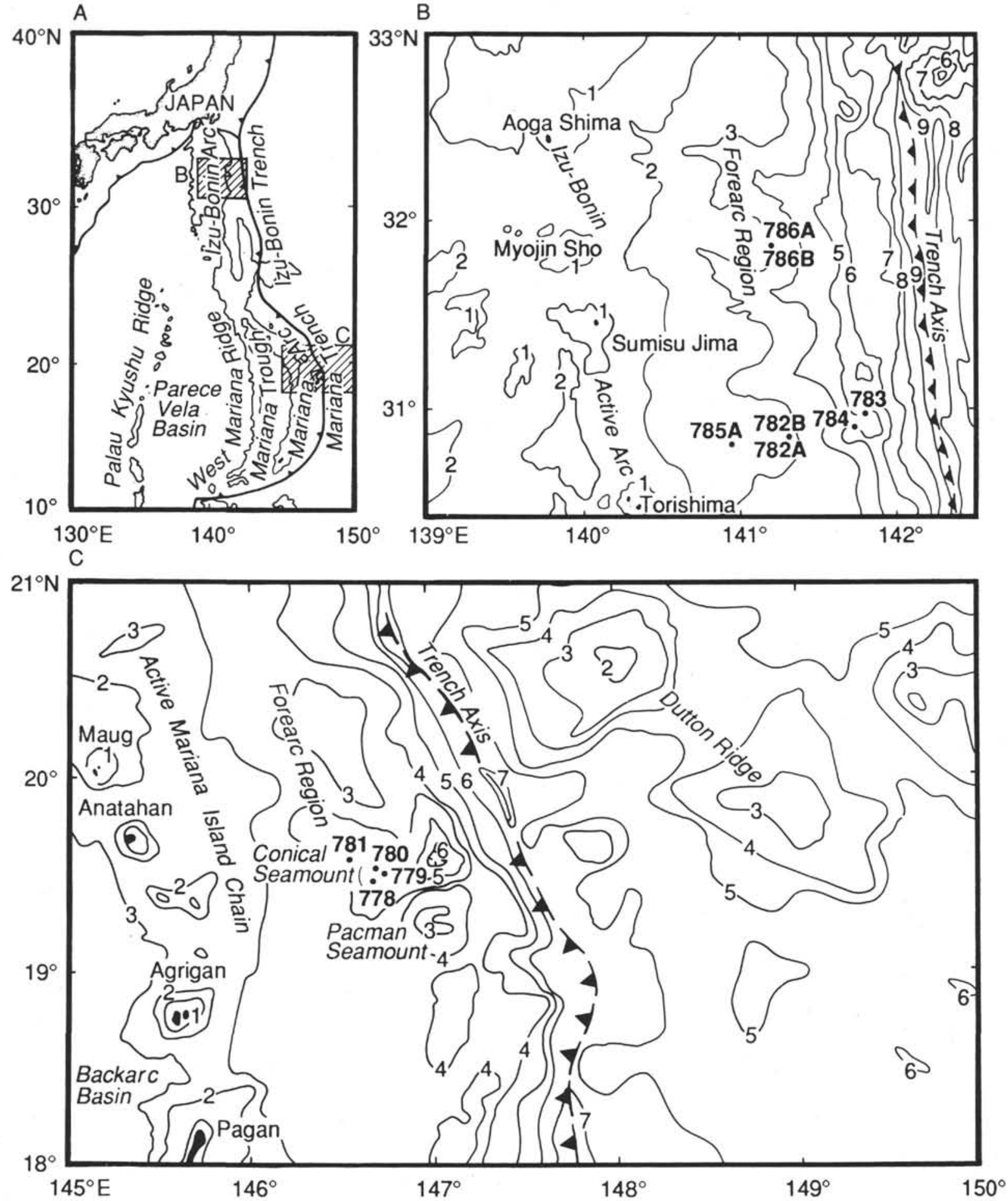


Figure 1. Location of ODP Leg 125 sites. **A.** Regional setting of Leg 125; shaded areas indicate locations of Figures 1B and 1C. **B.** Sites in the Izu-Bonin forearc region, including those drilled on Torishima Forearc Seamount (Sites 783 and 784). **C.** Sites in the Mariana forearc region, including those drilled on Conical Seamount (Sites 778–781). Contour interval in kilometers.

tures of serpentinite seamounts and to magnetic anomalies in forearc regions and show how this contribution depends on the degree of serpentinization.

# LITHOSTRATIGRAPHY AND PETROGRAPHY

## Sediment Classification

The textures and compositions of deposits of serpentine sediment suggested to Leg 125 scientists that the serpentine was emplaced as cold gravitational flows (Fryer, Pearce, Stokking, et al., 1990; Mottl and Haggerty, this volume; Fryer and Mottl, this volume; Phipps and Ballotti, this volume). The classification of serpentine sediments employed during Leg 125 is used in this study (see "Explanatory Notes" chapter of Fryer, Pearce, Stokking, et al., 1990, for detailed explanation). According to this classification scheme, the name "serpentinite" is restricted to lithified or indurated serpentine. The principal name of a sediment recovered during Leg 125 is "serpentine" if the sediment contains at least 60% of that mineral. Textural modifiers such as "sand-sized" or "silt-sized" precede the principal name, as appropriate. "Sheared phacoidal serpentine" comprises scales and chips of serpentine $\geq$ 1 mm. The anastomosing foliation of the sediment is produced by the orientation of the long axes of these particles; this sediment matrix may contain clasts of serpentinite $\geq$1 cm in diameter. Material containing large clasts in a finer-grained matrix is named "serpentine breccia," although no tectonic or sedimentary processes are implied.

## Lithostratigraphy

### *Site 778: Conical Seamount, Southern Flank*

The following lithostratigraphic units are described from Site 778 (Fryer, Pearce, Stokking, et al., 1990):

Subunit IA (0–7.2 m below seafloor, or mbsf) consists of serpentine-rich sediment (lower to middle Pleistocene to Holocene?) and serpentine flows that overlie serpentine clay, silt-sized serpentine, and serpentine-marl breccia.

Subunit IB (7.2–299.8 mbsf) contains sandy marl (lower to middle Pleistocene) with cobbles and pebbles of serpentinite and volcanic rocks.

Unit II (29.8 –107.6 mbsf) consists of sheared phacoidal serpentine (Pl. 1, Fig. 1) with a matrix that contains serpentine, magnetite, epidote-group minerals, chlorite, talc, and olivine. Within the sediment are clasts of variably serpentinized harzburgites and dunites, as well as clasts of mafic rocks. Modal estimates of the primary composition of the serpentinized peridotites are olivine (70%–95%), orthopyroxene (5%–30%) in which 1% to 2% clinopyroxene can be observed as exsolution lamellae, and chromium-spinel (Fryer, Pearce, Stokking, et al., 1990, pp. 102–103).

### *Site 779: Conical Seamount, Southeast Flank*

Three lithostratigraphic units were described from Site 779 (Fryer, Pearce, Stokking, et al., 1990):

Unit I (0–10.6 mbsf in Hole 779A) comprises unconsolidated sediments and flows of serpentine sediment early Pleistocene to Holocene in age.

Unit II (10.6–303.0 mbsf) is late Miocene to early Pleistocene in age and consists of sheared phacoidal serpentine that contains blocks and clasts of serpentinized harzburgite and dunite, along with mafic clasts and detrital serpentine sediments. The primary mineralogy of the serpentinized harzburgite, based on modal estimates (Fryer, Pearce, Stokking, et al., 1990, p. 122), is olivine (75%–85%), orthopyroxene (10%–25%), clinopyroxene (1%), and spinel (1%). That of the dunites is olivine (90%–99%), orthopyroxene (1%–10%), clinopyroxene (1%), and spinel (1%).

Unit III (303.0–317.2 mbsf) is a serpentine breccia.

### *Site 780: Conical Seamount, Summit*

Site 780 contains two lithostratigraphic units (Fryer, Pearce, Stokking, et al., 1990):

Unit I (0–14.0 mbsf in Hole 780C) comprises primarily middle Pleistocene(?) to Holocene(?) sand- and silt-sized serpentine.

Unit II (14.0–163.5 mbsf in Hole 780C) is a matrix of sandy silt-sized serpentine containing intervals of serpentinized peridotites. The primary mineralogy of the serpentinized peridotites from modal estimates is (Fryer, Pearce, Stokking, et al., 1990, p. 153) olivine (75%–90%), orthopyroxene (10%–25%), chromium-spinel (trace–2%), and clinopyroxene (trace–2%).

### *Site 784: Torishima Forearc Seamount, Western Flank*

Two lithostratigraphic units were described at Site 784 (Fryer, Pearce, Stokking, et al., 1990):

Subunits IA and IB (0–302.7 mbsf) consist of middle Miocene to upper Pleistocene vitric claystone and vitric silty clay.

Subunit IC (302.7–321.1 mbsf) comprises claystone and silt-sized serpentine.

Unit II (9321.1–425.3 mbsf) is a microbreccia of sheared phacoidal serpentine with clasts and blocks of serpentinized harzburgite (Pl. 1, Fig. 2), for which the primary mineralogy from modal estimates is (Fryer, Pearce, Stokking, et al., 1990, p. 278) olivine (65%–90%), orthopyroxene (10%–30%), clinopyroxene (trace–4%), and chromium-spinel (trace–2%). Extensively serpentinized clasts of dunite are also present.

## Oxide Petrography

### *Conical Seamount (Sites 778, 779, and 780)*

Serpentinized peridotites from the Conical Seamount sites contain from 1% to 3% magnetite and are <0.05 to 0.3 mm in diameter. Magnetite replaces chromium-spinel (Pl. 2, Figs. 1 and 2), orthopyroxene (Pl. 2, Fig. 3), and olivine. This mineral is concentrated in serpentine veins (Pl. 1, Fig. 3, and Pl. 2, Fig. 4) or occurs as dusty grains intergrown with serpentine and disseminated throughout the thin sections. In some samples, elongate stringers of <0.05-mm magnetite grains were observed to parallel felted blades of antigorite and fibers of chrysotile (Fryer, Pearce, Stokking, et al., 1990, p. 102). Magnetite in serpentinized dunite also was observed as rims outlining olivine and, in some samples, is associated with brucite.

Chromium-spinels in serpentinized harzburgites and dunites from Site 778 were identified from their translucent red color in transmitted light and are millimeters in diameter, although elongate grains up to 2 mm in length were observed at Site 780 (Fryer, Pearce, Stokking, et al., 1990, p. 153). Grains are disseminated, although some disseminated grains form bands up to 10 mm wide, and some grains occur in elongate trains. Grains are euhedral to subhedral, and some dumbbell shapes were observed. Chromium-spinel has been partially to completely altered to magnetite. Partially altered spinels from Site 779 contain unaltered cores that are translucent and rich in chromium and have been rimmed by magnetite and radiating halos of microcrystalline chlorite (Fryer, Pearce, Stokking, et al., 1990, p. 121; Saboda et al., this volume).

### *Torishima Forearc Seamount (Site 784)*

The occurrence of both magnetite and chromium-spinel in serpentinized peridotites from the Torishima Forearc Seamount is similar to that at Conical Seamount. Magnetite grains range from <0.05 to 0.3 mm in diameter and are concentrated in veins and disseminated throughout the sample; in addition, we observed these grains along cleavages of orthopyroxene and concentrated along boundaries among olivine, orthopyroxene, and clinopyroxene. However, the abundance of magnetite is greater here than at Conical Seamount, and ranges from trace amounts to 10%–15%.

## METHODS

Samples studied include both serpentinized peridotites and serpentine sediments from Holes 778A, 779A, and 780C at Conical Seamount and from Hole 784A at the Torishima Forearc Seamount. Samples of serpentinized peridotites were obtained aboard *JOIDES Resolution* by drilling minicores (about 12.4 $cm^3$) perpendicular to the split face of the core. These samples were oriented with respect to the upcore direction and were chosen to reflect increasing degrees of serpentinization, assessed on the basis of petrographic study. Sediment samples were taken aboard ship by pressing a 7-$cm^3$ plastic box into the split-core face with the sample oriented with respect to the upcore direction. The samples were shipped to Texas A&M University, where they are stored in $\mu$-metal containers.

The identification and characterization of the magnetic minerals were based on measurements of volume magnetic susceptibility and magnetic remanence, thermomagnetic analysis, acquisition of saturation isothermal remanence, coercivity of saturation remanence, thermal and alternating field demagnetization, and reflected- and transmitted-light microscopy.

Thermomagnetic analysis of 14 serpentinized peridotite samples was performed in an argon atmosphere using a vertical Curie balance at the Paleomagnetics Laboratory at the Scripps Institution of Oceanography. Magnetic susceptibilities were determined using a Bartington susceptibility meter (Model MS-1) from the Department of Oceanography, Texas A&M University. The intensities of the natural remanent magnetization (NRM) of the samples were measured on a three-axis CTF cryogenic magnetometer housed in a shielded room in the Paleomagnetics Laboratory at the Department of Geophysics, Texas A&M University. This instrument provides a value of the total magnetic moment of the sample ($Am^2$) and has a noise level of approximately $10^{-11}$ $Am^2$. Alternating field (AF) demagnetization of the samples was performed using a Schonstedt AF demagnetizer. Samples were measured in the cryogenic magnetometer between AF steps. Four samples for which the intensity did not decay to zero remanence during AF demagnetization were also thermally demagnetized using a Schonstedt thermal demagnetizer and then measured in the cryogenic magnetometer, but heating caused minerals in the samples to alter to hematite, rendering the demagnetization data unreliable.

Saturation isothermal remanence (SIRM) was imparted to the samples by applying increasing impulse fields (0 to 1.0 T) using an impulse magnetizer constructed for ODP by ASC, Inc. The coercivity of saturation remanence ($H_{CR}$) of the samples was determined by applying an increasing reverse-field isothermal remanent magnetization (IRM) to the samples. A second SIRM was demagnetized using the Schonstedt AF demagnetizer so that the demagnetization behavior of NRM could be compared to that of SIRM. The SIRM intensity of the samples was too strong to permit their measurement in the cryogenic magnetometer, so the samples were measured in a Molspin spinner magnetometer, which provides a measurement of volume magnetic moment (A/m).

The volumes of 14 minicore samples were calculated using a Quantachrome Penta-Pycnometer, which determines volume based on the displacement of gaseous helium. Volumes and weights were measured both before and after freeze-drying the samples for 24 hr. Densities determined after freeze-drying averaged 0.4% greater than those determined before freeze-drying. To avoid mineral alteration, the samples were not oven dried. Volume also was determined by taking multiple measurements of the dimensions of the samples; volume calculated by this method differed systematically from that determined in the pycnometer by about 4%. The volume measurements (before freeze-drying) were used to normalize magnetic susceptibility, to calculate density, and to convert remanence measured on the cryogenic magnetometer from total moment ($Am^2$) to volume moment (A/m) for comparison with data from the spinner magnetometer and for use in determining the Koenigsberger ratio ($Q$).

Koenigsberger ratios ($Q_{NRM}$) were calculated based on $Q_{NRM} = M_{NRM}/kH$, where $M_{NRM}$ is the NRM of the sample, $k$ is the volume susceptibility (which is unitless in the SI system), and $H$ is Earth's field at the site (e.g., Collinson, 1983). The values of $H$ used here are 31.83 A/m (40,000 nT) for Sites 778, 779, and 780 at Conical Seamount and 35.01 A/m (44,000 nT) for Site 784 at Torishima Forearc Seamount (Merrill and McElhinny, 1983).

Polished thin sections were prepared by Mid-West Petrographics and were studied using a Zeiss photomicroscope.

Hysteresis properties of the samples were not measured because an operational instrument was not available.

## RESULTS

### Density

Grain densities of serpentinized peridotites (determined using volumes measured in the pycnometer) range from 2.44 to 3.02 $g/cm^3$ before freeze-drying, with a mean of 2.68 $g/cm^3$; after freeze-drying densities range from 2.47 to 3.02 $g/cm^3$, with a mean of 2.69 $g/cm^3$. Densities (based on multiple dimension measurements from six additional samples) range from 2.19 to 3.00 $g/cm^3$. The densities of these samples of serpentinized peridotite are presented in Table 1.

### Rock Magnetic Properties

The NRM intensity of the serpentinized peridotites ranges from 0.01 to 0.59 A/m (mean: 0.20 A/m); Table 1 presents the rock magnetic properties of serpentinized peridotites, and Table 2 presents those of serpentine sediments. Volume susceptibilities of serpentinized peridotites (with the exception of an anomalously high value of 80.93, measured in a serpentinized dunite) range from $0.05 \times 10^{-3}$ SI to $9.78 \times 10^{-3}$ SI (mean: $3.83 \times 10^{-3}$ SI) and Koenigsberger ratios vary from 0.09 to 4.49 (mean: 1.71). The NRM intensity of serpentine sediments ranges from 0.01 to 0.43 A/m (mean: 0.07 A/m), volume susceptibilities range from $0.12 \times 10^{-3}$ to $4.34 \times 10^{-3}$ SI (mean: 2.08 $\times 10^{-3}$ SI), and Koenigsberger ratios from 0.06 to 4.74 (mean: 1.43). The coercivity of saturation remanence of serpentinized peridotites ranges from 14 to 50 mT and that of serpentine sediments ranges from 21 to 81 mT.

Representative thermomagnetic diagrams are presented in Figure 2. Although the samples were analyzed in an argon atmosphere, the release of structural water and/or hydroxyl from the samples during heating caused the minerals to alter (probably to hematite) while determining the Curie temperatures. The curves therefore are not reversible (Fig. 2A). Nonetheless, measurement of three samples of serpentinized harzburgite (125-778A-9R-1, 9–11 cm, 125-779A-5R-1, 131–133 cm, and 125-779A-22R-1, 78–80 cm) produced curves typified by Figure 2B, in which most of the magnetization is lost by 580°C, which is characteristic of iron-end-member magnetite; however, a small percentage persists to higher temperatures, suggesting the presence of hematite that probably was produced by alteration during heating.

The decay of intensity of remanence during progressive AF demagnetization provides an indication of the coercivity spectrum of the rock, a property that, assuming the sample contains only one component of remanence and a single type of magnetic carrier, is itself dependent on the grain-size spectrum in the rock. The AF demagnetization behavior of representative samples of serpentinized peridotites is illustrated in Figures 3A through 3H. All serpentinized peridotite samples followed one of four types of demagnetization behavior. A single component of remanence can be isolated in type 1 samples. The median destructive field (MDF, the field required to reduce the NRM to one-half) of these samples ranges from 4.5 to

**Table 1. Rock magnetic properties of serpentinized peridotites from Leg 125.**

| Core, section, interval (cm) | Lithologic unit | Density ($g/cm^3$) | Natural remanent magnetization (A/m) | Median destructive field[a] (mT) | Volume susceptibility ($10^{-3}$ SI) | Koenigsberger ratio (SI) | Intensity of saturation isothermal remanence (A/m) | Saturation field (mT) | Coercivity of saturation remanence (mT) |
|---|---|---|---|---|---|---|---|---|---|
| 125-778A- | | | | | | | | | |
| 2R-1, 104–106 | Bastite | 2.44 | 0.10 | 37.5 (3) | 1.97 | 1.59 | 71.97 | 154 | 42 |
| 8R-1, 55–57 | Serpentinite | 2.49 | 0.36 | 5.5 (1) | 4.97 | 2.28 | 499.4 | 130 | 29 |
| 9R-1, 9–11 | Serpentinized harzburgite | [b]– | 0.21 | 32.5 (3) | 1.30 | 5.08 | | | |
| 125-779A- | | | | | | | | | |
| 5R-1, 131–133 | Serpentinized harzburgite + dunite | 2.62 | 0.24 | 6.0 (1) | 2.81 | 2.68 | 249.1 | | 19 |
| 14R-1, 81–83 | Serpentinized harzburgite | 2.82 | 0.59 | 7.2 (1) | 9.94 | 1.86 | 448.0 | 51 | 22 |
| 22R-1, 78–80 | Serpentinized harzburgite | 2.80 | 0.27 | 7.0 (1) | 5.72 | 1.48 | 69.7 | 250 | 22.5 |
| 25R-1, 73–7500 | Serpentinized dunite | [b]2.46 | 0.09 | 6.0 (1) | 8.60 | 0.09 | 70.3 | 222 | 30 |
| 26R-1, 69–71 | Serpentinized harzburgite | 2.72 | 0.54 | 2.0 (2) | 6.54 | 2.59 | 140.8 | 228 | 30 |
| 26R-3, 71–73 | Serpentinized harzburgite | 2.67 | 0.02 | 18.0 (3) | 2.54 | 0.25 | 24.3 | 234 | 38 |
| 28R-3, 65–67 | Serpentinized harzburgite | [b]2.93 | 0.01 | >100 (3) | 1.14 | 0.28 | | | |
| 31R-1, 21–23 | Serpentinized dunite | 2.69 | 0.01 | 4.9 (1) | 0.07 | 4.49 | 6.4 | 134 | 27 |
| 32R-3, 23–25 | Serpentinized harzburgite | [b]2.71 | 0.12 | 2.0 (2) | 1.96 | 1.92 | 20.99 | 336 | 36 |
| 125-780C- | | | | | | | | | |
| 6R-1, 85–87 | Serpentinized harzburgite | 2.66 | 0.41 | 2.5 (2) | 8.41 | 1.53 | 156.1 | 200 | 25 |
| 9R-1, 56–58 | Serpentinized harzburgite | [b]2.61 | 0.07 | 2.0 (2) | 3.52 | 0.63 | 37.2 | 202 | 29 |
| 13R-1, 56–59 | Serpentinized harzburgite | 3.02 | 0.37 | 8.0 (1) | 9.78 | 1.19 | 302.9 | 112 | 22.5 |
| 18R-1, 105–107 | Serpentinized harzburgite | 2.77 | 0.09 | 8.0 (1) | 3.63 | 0.78 | 73.5 | 179 | 19 |
| 125-784A- | | | | | | | | | |
| 38R-1, 147–149 | Serpentinized harzburgite | [b]– | 0.13 | 7.0 (1) | 2.97 | 1.25 | 73.2 | 132 | 14 |
| 40R-2, 52–54 | Serpentinized dunite | 2.55 | 0.17 | 32.0 (3) | 0.06 | 80.93 | 463.3 | 125 | 33 |
| 42R-1, 50–52 | Serpentinized harzburgite + dunite | [b]– | 0.03 | 10.0 (3) | 2.73 | 0.31 | | | |
| 44R-1, 31–34 | Serpentinized harzburgite | [b]– | 0.25 | 4.5 (1) | 2.11 | 3.34 | | | |
| 45R-1, 33–35 | harzburgite | [b]2.19 | 0.53 | 6.0 (1) | 3.63 | 4.17 | 87.1 | 245 | 21 |
| 45R-1, 140–143 | harzburgite | [b]3.00 | 0.02 | 6.0 (1) | 2.29 | 0.25 | | | |
| 45R-2, 22–25 | Serpentinized harzburgite | 2.60 | 0.05 | 9.5 (1) | 1.80 | 0.79 | 28.3 | 365 | 43 |
| 45R-2, 67–71 | Serpentinized harzburgite | 2.61 | 0.05 | 52.0 (4) | 3.49 | 0.41 | 36.3 | 316 | 50 |

[a] Numbers in parentheses refer to type of demagnetization behavior.
[b] Volume calculated by multiple measurements of sample dimensions.

9.5 mT. A single component of remanence can be isolated from type 2 samples as well, but the MDF of these samples is less than 2.5 mT. The third type (type 3) of behavior is exhibited by samples that contain more than one component of remanence. AF demagnetization techniques cannot reduce the NRM to zero intensity and vector-end-point plots of the demagnetization data indicate opposing remanence components. The MDF of these samples ranges from 10 to >100 mT. The fourth type of behavior (type 4) is exhibited by a single sample for which the NRM can be demagnetized using AF techniques, but which has a high MDF (52.0 mT).

The AF demagnetization behavior of serpentine sediments is illustrated in Figures 4A through 4F. Most sediment samples contain a single component of remanence that can be isolated by AF techniques; the MDF of most sediment samples ranges from 2.0 to 10.2 mT. However, the demagnetization behavior of Sample 125-779A-37R-1, 12–14 cm, differs from that of the other sediment samples and is not similar to the behavior of any of the serpentinized peridotite samples. Although a single component of remanence was exhibited (Fig. 4F), AF demagnetization to 100 mT removes only 60% of the NRM (MDF: 52 mT).

The IRM acquisition behavior of representative serpentinized peridotite samples is illustrated in Figure 5. Samples become saturated at applied fields of between 51 and 365 mT. The intensity of SIRM varies considerably, ranging from 6.4 to 499.4 A/m. The variation does not appear to be related to depth or to differences in lithology. The IRM acquisition behavior of serpentine sediments is

**Table 2. Rock magnetic properties of serpentine sediments from Leg 125.**

| Core, section interval (cm) | Lithologic unit | Natural, remanent magnetization (A/m) | Median destructive field (mT) | Volume susceptbility ($10^{-3}$ SI) | Koenigsberger ratio (SI) | Intensity of saturation isothermal remanence (A/m) | Saturation field (m/T) | Coercivity of saturation remanence (m/T) |
|---|---|---|---|---|---|---|---|---|
| 125-778A- | | | | | | | | |
| 7R-1, 39–41 | Sheared phacoidal serpentine | 0.02 | 5.5 (1) | 4.34 | 0.15 | | | |
| 11R-1, 131–133 | Sheared phacoidal serpentine | 0.01 | 10.2 (1) | 2.58 | 0.17 | 44.3 | 125 | 21 |
| 125-779A- | | | | | | | | |
| 37R-1, 12–14 | [b]Silty serpentine | 0.01 | 52.0 (D) | 0.12 | 3.40 | 0.13 | 316 | 81 |
| 125-784A- | | | | | | | | |
| 35R-2, 25–27 | Silty serpentine | 0.10 | 4.0 (I) | 2.23 | 1.24 | | | |
| 35R-CC, 8–10 | Silty serpentine | 0.01 | 6.0 (1) | 1.08 | 0.16 | | | |
| 37R-1, 25–27 | Serpentine breccia | 0.06 | 3.0 (I) | 2.75 | 0.62 | | | |
| 38R-1, 39–41 | Sheared phacoidal serpentine | 0.01 | 6.0 (1) | 2.97 | 0.06 | 3.7 | 112 | 62 |
| 39R-1, 130–132 | Sheared phacoidal serpentine | 0.01 | 2.0 (I) | 0.13 | 2.20 | | | |
| 41R-2, 84–86 | Sheared phacoidal serpentine | 0.08 | 4.5 (1) | 3.97 | 0.58 | | | |
| 43R-1, 26–29 | Sheared phacoidal serpentine | 0.08 | 4.5 (1) | 1.17 | 1.95 | | | |
| 43R-1, 90–93 | Sheared phacoidal serpentine | 0.06 | 22.0 (4) | 0.58 | 2.96 | 16.3 | 563 | 62 |
| 43R-2, 91–93 | Sheared phacoidal serpentine | 0.03 | 4.5 (1) | 2.55 | 0.34 | | | |
| 43R-3, 41–43 | Sheared phacoidal serpentine | 0.43 | 4.2 (I) | 2.59 | 4.74 | 45.5 | 317 | 21 |

Note: All volumes assumed to be 7 $cm^3$.
[a]Numbers in parentheses indicate similarity to type of demagnetization behavior exhibited by serpentinized peridotites; I = behavior intermediate between that of type 1 and type 2 serpentinized peridotites, D = demagnetization behavior different from serpentinized peridotites.
[b]Chlorite-rich and thulite-bearing.

illustrated in Figure 6. Saturation (of five samples) was obtained by applied fields of between 125 and 563 mT, and saturation intensity ranges from 0.13 to 45.4 A/m.

## DISCUSSION

### Magnetic Carrier

Petrographic observations revealed at least two modes of occurrence of magnetite in the serpentinized peridotites from Leg 125: (1) very fine-grained "dusty" magnetite disseminated throughout the rock and intergrown with serpentine and clay and (2) very fine-grained and coarser grained (up to 0.3 mm) magnetite associated with serpentine in veins. This roughly bimodal distribution of grain sizes is reflected by the magnetic properties of the peridotites. Behavior during AF demagnetization and acquisition of IRM were characteristic of magnetite; the Curie temperatures that were obtained are typical of iron-end-member magnetite. The grain-size variation observed is reflected by the two predominant types of AF demagnetization behavior: the most frequently observed behavior (type 1), characterized by MDFs between 4.5 and 9.5 mT, is exhibited by samples that contain finer grained magnetite than the type 2 samples, which have MDFs <2.5 mT. Type 3 samples contain more than one component of remanence. The coercivity of the magnetic carrier in type 4 samples is greater than that of types 1 and 2, suggesting that it is either higher coercivity mineral. Additional petrographic and geochemical studies are required to resolve this point. The variation in saturation remanence (Figs. 5 and 6) reflects differences in both grain size and amount of magnetite.

### Type of Remanence

A single component of remanence can be isolated from many of the samples characterized by MDFs of less than 9.5 mT. This component represents a chemical remanent magnetization (CRM) acquired by particles of magnetite as they form during serpentinization (Burch, 1965). In addition, the low stability of most samples suggests that at least some of the remanence might be viscous (VRM; studies of VRM acquisition are planned). Evidence from fluids indicates that serpentinization at Conical Seamount is still going on (Fryer, Pearce, Stokking, et al., 1990; Fryer and Mottl, this volume; Mottl and Haggerty, this volume), but the deformed nature of the peridotites and their occurrence as clasts and blocks within zones of serpentine sediments make interpretation of their directional properties impossible. The timing of the acquisition of remanence and its relationship to the history of the seamount therefore cannot be determined.

### AF Demagnetization of SIRM

The saturation IRM of several samples was demagnetized so that the characteristics of demagnetization of NRM could be compared to those of the demagnetization of SIRM (Lowrie and Fuller, 1971; Fuller et al., 1988). The demagnetization behavior of serpentinized peridotites is illustrated in Figures 7A and 7B and that of serpentine sediments is illustrated in Figure 7C. Lowrie and Fuller (1971) showed that for magnetite the relative stability of SIRM and NRM (assuming that it is a thermoremanent magnetization, or TRM) can be used to evaluate the domain state that predominates in the primary

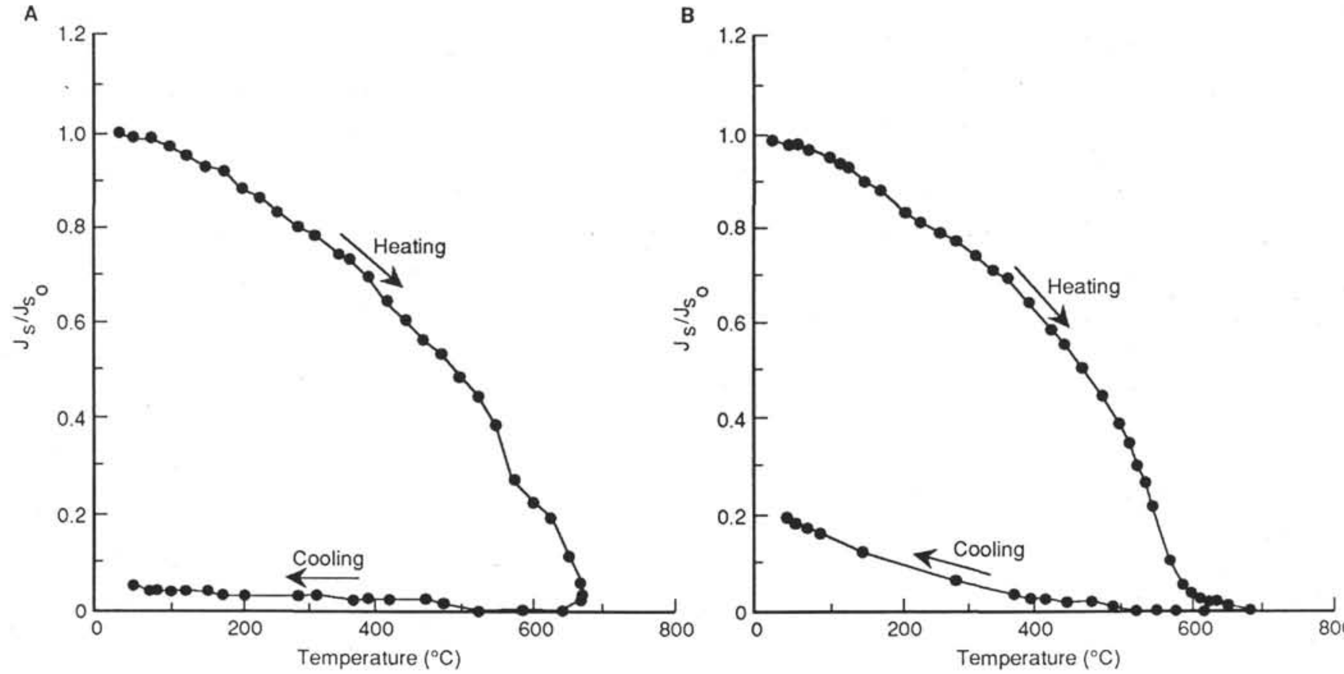


Figure 2. Thermomagnetic behavior of (**A**) Sample 125-778A-2R-1, 104–106 cm, and (**B**) Sample 125-778A-2R-1, 9–11 cm. The heating rate was 10° per minute.

carrier of remanence in a sample. Because CRM and TRM are acquired in a similar manner, theory predicts that their properties will be similar (Stacey and Banerjee, 1974). This has been demonstrated for hematite by Stokking and Tauxe (1990) and for magnetite by Pick and Tauxe (1991); the similarities between TRM and CRM suggest that the Lowrie-Fuller test may be applicable to rocks that contain CRM carried by magnetite. The presence of single-domain grains of magnetite cannot be evaluated petrographically: the transition from single-domain to multidomain behavior in magnetite occurs at grain sizes on the order of 0.5 μm. Thus, single-domain and small multidomain particles cannot be observed using light microscope.

The SIRM of Sample 125-779A-26R-1, 69–71 cm (Fig. 7A), a serpentinized harzburgite, is more stable than that of its NRM, which implies that the magnetization of the sample is dominated by multidomain material (Fuller et al., 1988; Lowrie and Fuller, 1971). Similar behavior was observed in a sheared phacoidal serpentine (Sample 125-784A-43R-3, 41–43 cm; Fig. 7C), which has an SIRM more stable than its NRM. The stability of the SIRM of Sample 125-784A-45R-2, 67–71 cm (Fig. 7B), a serpentinized harzburgite, is less than that of its NRM, suggesting that single-domain magnetite predominates (Lowrie and Fuller, 1971). In other samples of serpentinized peridotites, the distinction is less clear–SIRM and NRM stabilities are similar, perhaps because of roughly equal contributions from both single-domain and multidomain grains. Such variation should not be surprising: from the range of grain sizes observed at the thin-section level, single-domain, pseudo-single-domain, and multidomain grains might all be present.

## Comparison of Serpentine Sediments with Serpentinized Peridotites

The magnetic properties (NRM intensity, AF demagnetization behavior of NRM and SIRM, volume susceptibility, and Koenigsberger ratio) of serpentine sediments are remarkably similar to those of serpentinized peridotites. One possible explanation is that the magnetic carriers that predominate in the serpentinized peridotites persist relatively unchanged during sediment transport and are deposited such that their abundance in the sediments is approximately equal to that in the serpentinites from which they are derived. Another possibility is that the particles of magnetite are altered during transport to a mineral with magnetic properties that are similar to those of magnetite, such as maghemite. Additional petrographic and geochemical study including scanning electron microscope and electron microprobe analyses of the magnetic particles present in the serpentine sediments is planned and should resolve this question.

## Rock Magnetic Properties and Degree of Serpentinization

As serpentinization progresses, the density of the rock decreases (Coleman, 1971); plots of rock magnetic parameters vs. density might be expected to indicate how these properties change during serpentinization. Because magnetite is a product of serpentinization, one would expect that bulk magnetic properties, such as susceptibility, NRM, and saturation remanence, would increase as serpentinization proceeds. The variation of grain density with susceptibility is shown in Figure 8. Figures 9A and 9B illustrate the variation of grain density with NRM and SIRM intensity. The three plots all show a great deal of scatter, similar to a plot of susceptibility vs. density for several serpentinites and peridotites reported by Coleman (1971). The amount of magnetic material in a serpentinite depends not only on the degree of serpentinization, but on the abundance and composition of the parent minerals from which the magnetic material was derived (Luyendyk and Day, 1982; Shive et al., 1988). Therefore, simple linear relationships between density and magnetic properties should not be expected; the composition of the primary mineral assemblages must also be considered when assessing the changes of magnetic properties with increasing serpentinization.

A plot of susceptibility vs. NRM intensity (Fig. 10) is roughly linear, which indicates that the magnetic material responsible for the increases in susceptibility is capable of acquiring a remanent magnetization (i.e., is not superparamagnetic). Susceptibility is a measure of the amount of magnetite present in the serpentinized peridotites;

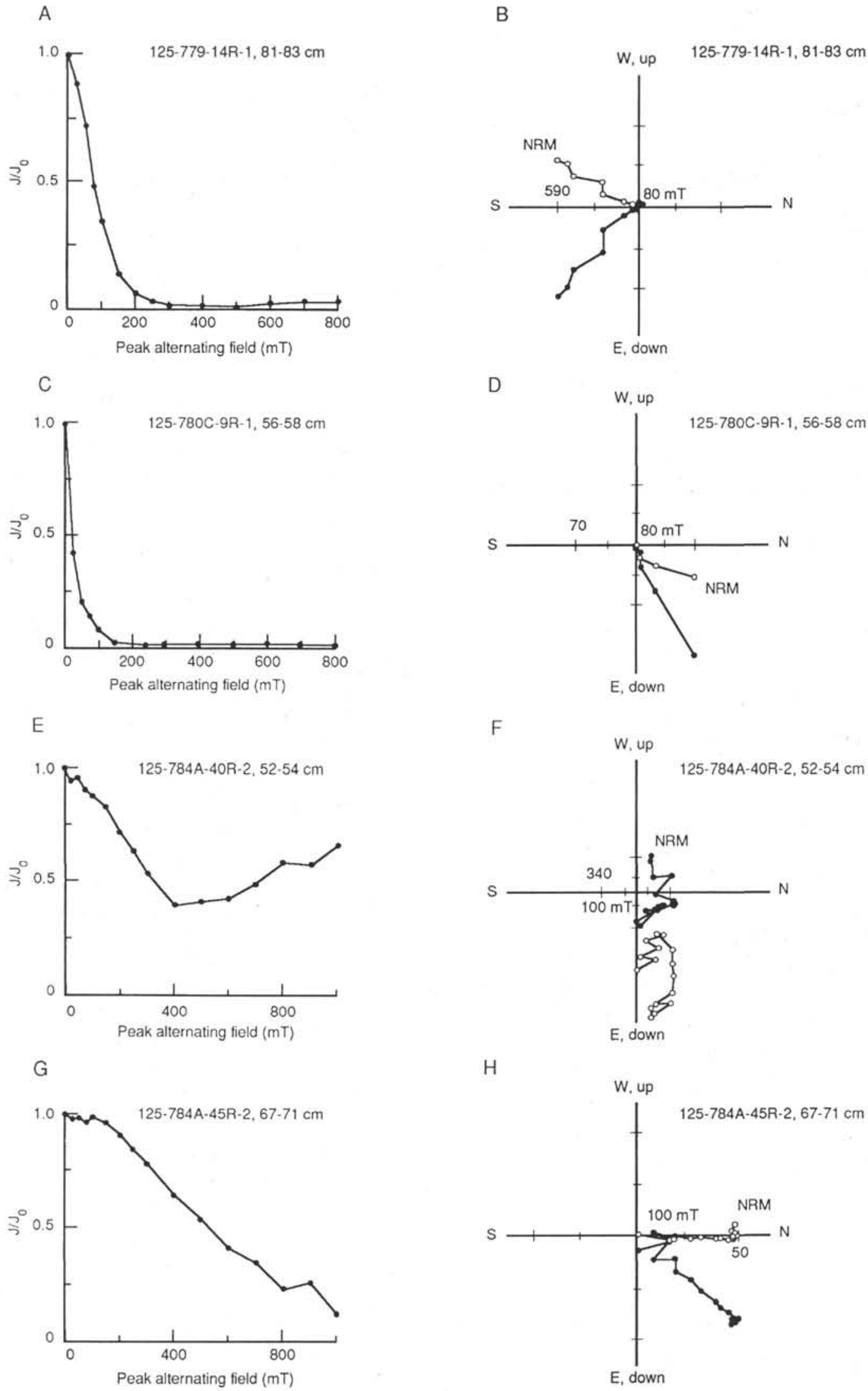


Figure 3. AF demagnetization behavior of serpentinized peridotites. Solid symbols represent the horizontal component of remanence and open symbols represent the vertical component. Intensity units are in mA/m. NRM and final peak demagnetizing field are indicated. **A.** Intensity decay (type 1). **B.** Vector-end-point diagram (type 1). **C.** Intensity decay (type 2). **D.** Vector-end-point diagram (type 2). **E.** Intensity decay (type 3). **F.** Vector-end-point diagram (type 3). **G.** Intensity decay (type 4). **H.** Vector-end-point diagram (type 4).

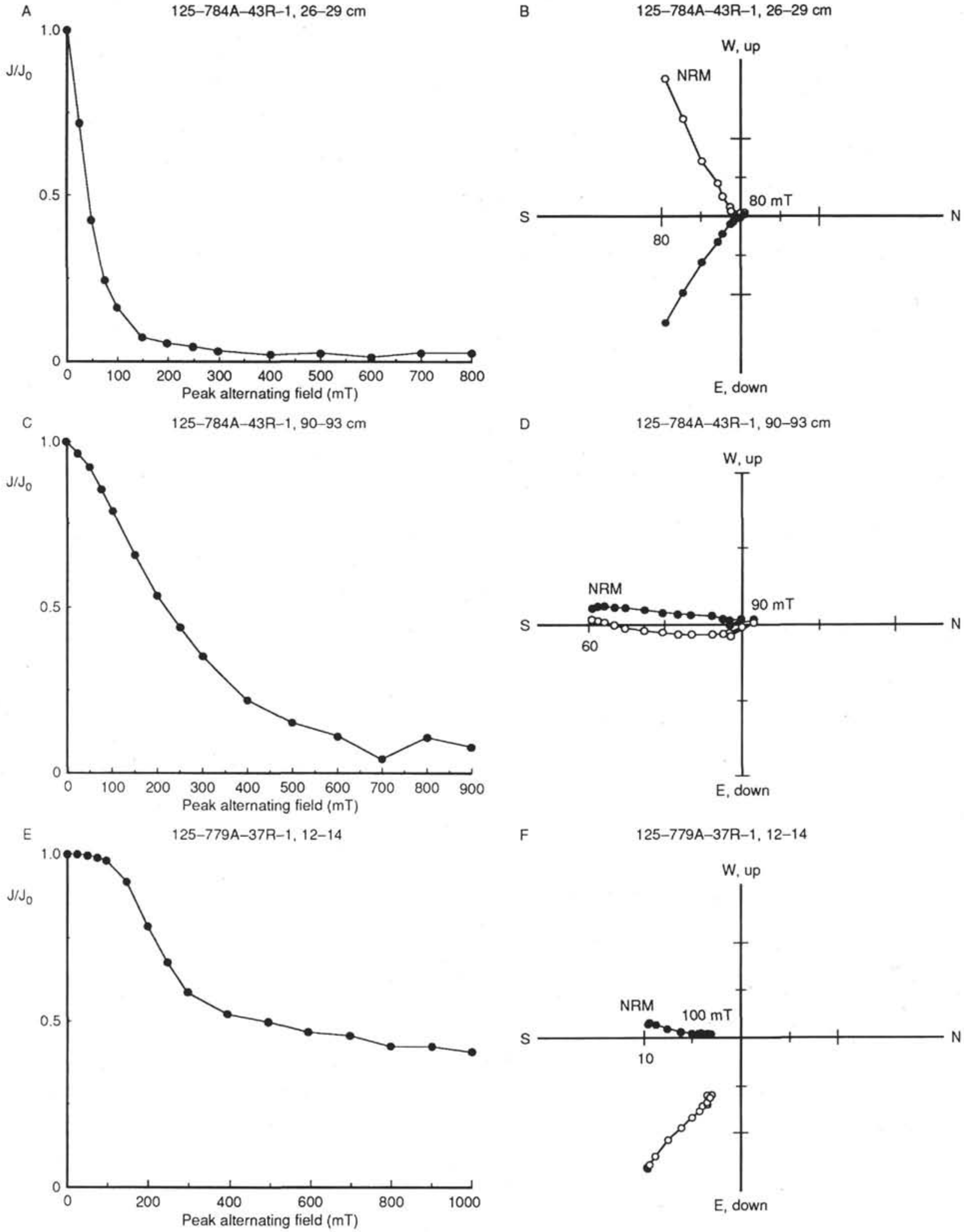


Figure 4. AF demagnetization behavior of serpentine sediments. See Figure 3 for explanation. **A.** Intensity decay (similar to type 1 serpentinized peridotites). **B.** Vector-end-point diagram (similar to type 1 serpentinized peridotites). **C.** Intensity decay (similar to type 4 serpentinized peridotites). **D.** Vector-end-point diagram (similar to type 4 serpentinized peridotites). **E.** Intensity decay. **F.** Vector-end-point diagram. The demagnetization behavior of this sample differs from that of samples of serpentinized peridotites and serpentine sediments.

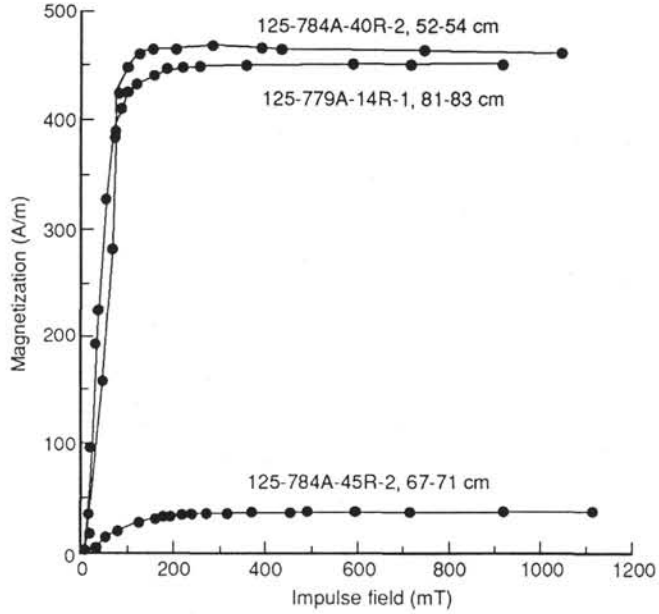


Figure 5. Behavior during acquisition of saturation IRM by serpentinized peridotites. Sample 125-779A-14R-1, 81–83 cm, is serpentinized harzburgite, Sample 125-784A-40R-2, 52–54 cm, is serpentinized dunite, and Sample 125-784A-45R-2, 67–71 cm, is serpentinized harzburgite.

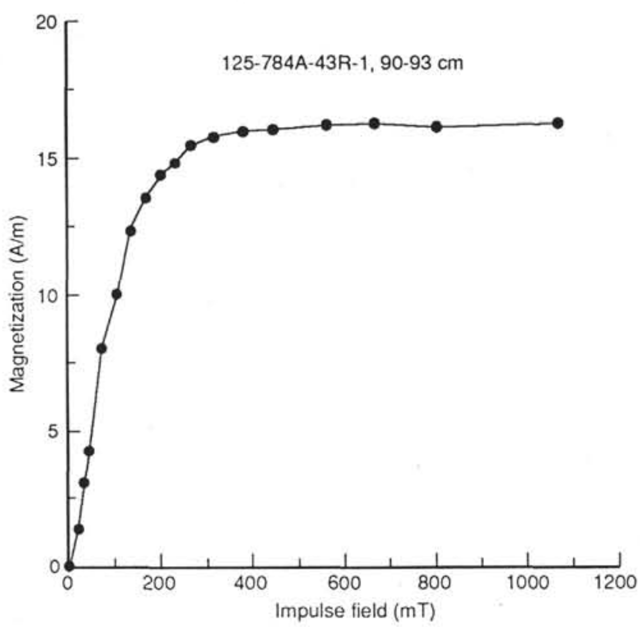


Figure 6. Behavior during acquisition of saturation IRM by serpentine sediments. Sample 125-784A-43R-1, 90–93 cm, is sheared phacoidal serpentine.

thus, we evaluate the variation of the IRM saturation field, coercivity of remanence, saturation remanence, and median destructive field with susceptibility (Figs. 11A–11D). As susceptibility increases, the saturation field and coercivity of remanence roughly decrease, and the saturation remanence tends to increase. These trends imply that lower coercivity (larger) grains predominate as magnetite abundance increases, which may reflect a greater abundance of coarser grained magnetite in veins relative to the dusty magnetite intergrown with serpentine disseminated throughout the rock. The scatter observed in a plot of MDF vs. susceptibility implies contributions from populations of different grain size and is a good illustration of the complexities of the serpentinite magnetization.

## Potential Contribution to Magnetic Anomalies

The potential contribution of serpentinized ultramafic rocks to the magnetic signature of serpentinite seamounts and to magnetic anomalies in general can be evaluated on the basis of remanence characteristics and Koenigsberger ratios (Tables 1 and 2). The NRM intensity of serpentinized peridotites ranges from 0.01 to 0.59 A/m (mean: 0.20 A/m), somewhat less than that of young mid-ocean ridge (Van Wagoner and Johnson, 1983) and seamount (Gee et al., 1988) basalts. Volume susceptibilities of serpentinized peridotites range from $0.05 \times 10^{-3}$ SI to $9.78 \times 10^{-3}$ SI (mean: $3.83 \times 10^{-3}$ SI; about an order of magnitude less than submarine basalts). Koenigsberger ratios vary from 0.09 to 4.49 (mean: 1.71). Values for $Q$ greater than 1 indicate that the remanent component exceeds the induced component of magnetization. Magnetic data from serpentinite seamounts will be useful for constructing models of magnetic anomalies in forearc regions.

## CONCLUSIONS

1. The magnetic behavior of serpentinized peridotites from forearc serpentinite seamounts is complex and reflects not only the process of serpentinization, but also the variability in the composition of the parent rock.

2. The range in size of magnetite particles in the serpentinized peridotites is reflected by differences in magnetic properties and stability. Magnetic carriers other than magnetite may be present in the system as well. Future research will involve scanning electron microanalysis and measurement of the hysteresis properties of the magnetic material in these rocks to constrain the range of particle sizes and domain states more accurately.

3. The magnetic properties of serpentine sediments are similar to those of serpentinized peridotites, either because the magnetite that predominates in the serpentinites persists in the sediments or because

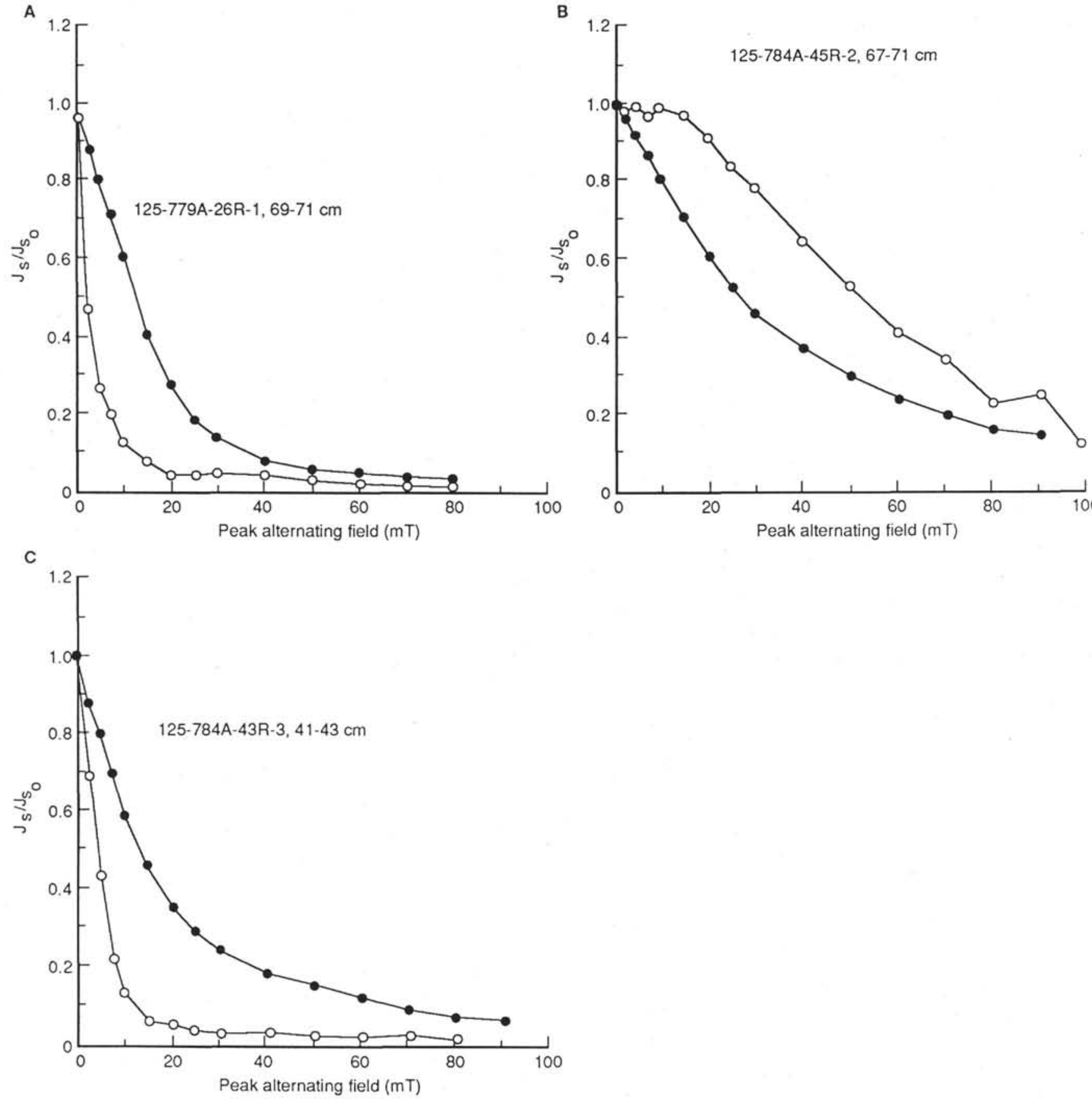


Figure 7. AF demagnetization behavior of SIRM (solid symbols) and NRM (open symbols) from samples of (**A** and **B**) serpentinized harzburgite and (**C**) sheared phacoidal serpentine.

it has altered to a mineral that has magnetic characteristics and an abundance similar to magnetite, such as maghemite.

4. Because of the complexity of both the magnetization of serpentinized peridotites and the process of serpentinization, and perhaps because the serpentinization is extensive, there is no simple correlation between degree of serpentinization and rock magnetic properties. Future research will involve electron microprobe analysis of the opaque minerals as well as the nonopaque spinels to assess the compositional variability of primary minerals and secondary magnetic material and to determine the role of this variability in serpentinite magnetization.

5. Magnetic data from serpentinized seamounts should be included in models of magnetic anomalies in forearc regions.

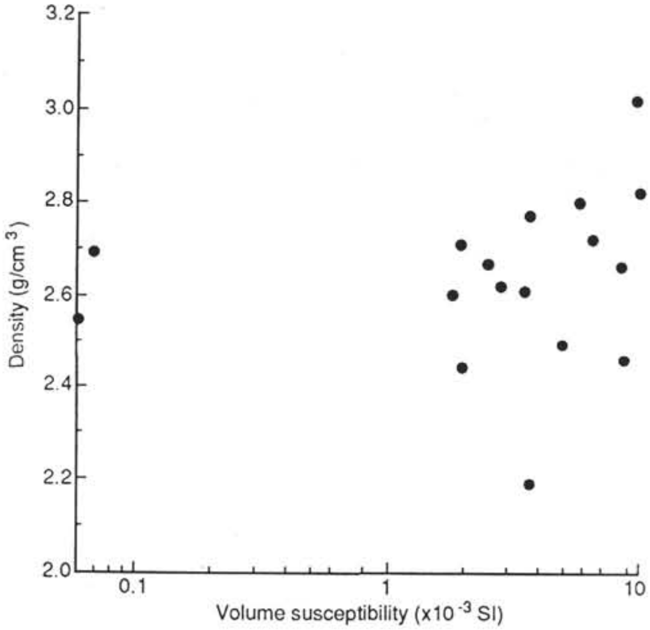


Figure 8. Volume magnetic susceptibility vs. density, serpentinized peridotites, Leg 125.

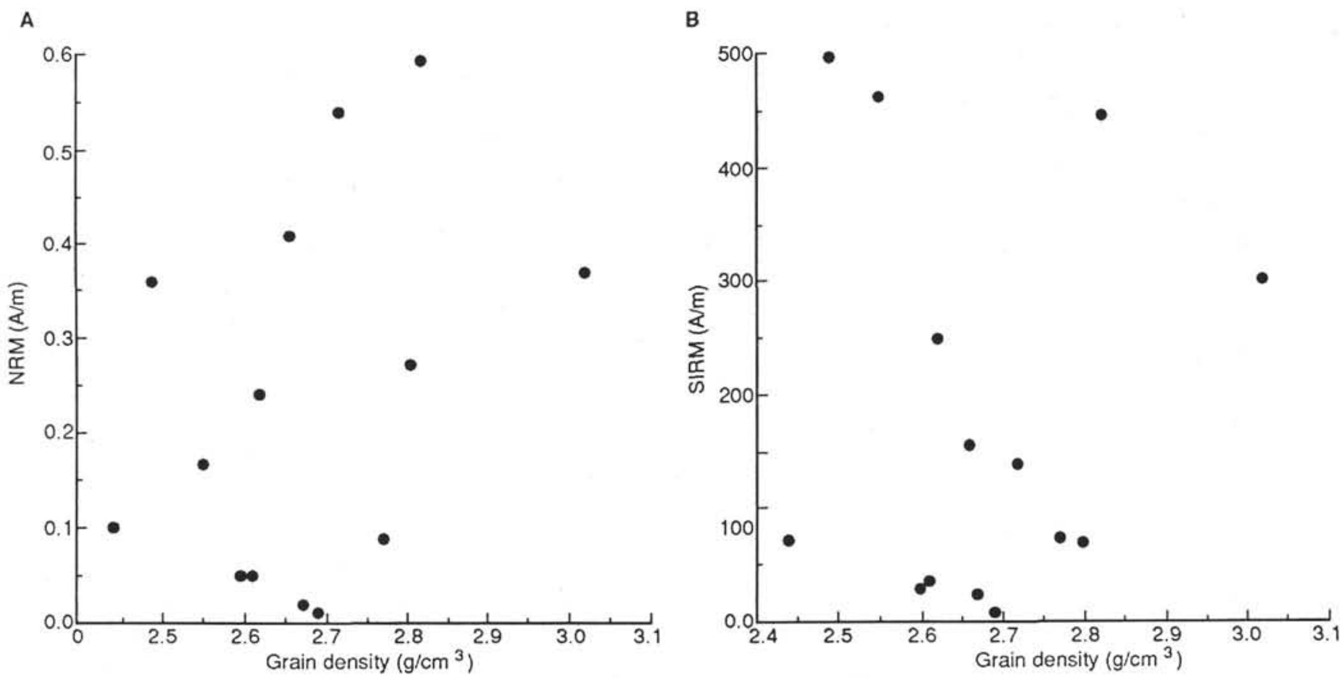


Figure 9. Grain density vs. (**A**) NRM intensity and (**B**) SIRM intensity, serpentinized peridotites, Leg 125.

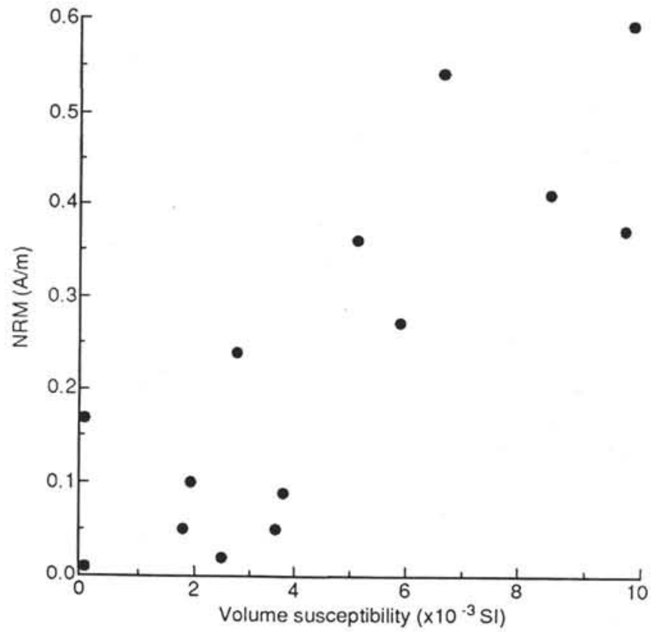


Figure 10. Volume susceptibility vs. NRM intensity, serpentinized peridotites,

## ACKNOWLEDGMENTS

We thank J. Aguiar for assistance with data processing, L. Tauxe for the use of her Curie balance and J. Gee for help with its operation, A. Fisher for help with pycnometer measurements, J. Allan for advice on reflected-light microscopy, and W. Sager for the use of his susceptibility meter. We are grateful to P. Coleman and G. Thrupp for their thoughtful reviews and helpful comments. This research was supported by a grant to L. S. from the U.S. Science Support Program of the Joint Oceanographic Institutions, Inc.

### REFERENCES

Banerjee, S. K., 1980. Magnetism of the oceanic crust: evidence from ophiolite complexes. *J. Geophys. Res.,* 85:3557–3566.

Beske-Diehl, S. J., and Banerjee, S. K., 1980. Metamorphism in the Troodos ophiolite: implications for marine magnetic anomalies. *Nature,* 285:563–564.

Bina, M. M., Henry, B., and Cannat, M., 1990. Magnetic anisotropy and some other magnetic properties of serpentinized peridotites from ODP Hole 670A. *In* Detrick, R., Honnorez, J., Bryan, W. B., Juteau, T., et al., *Proc. ODP, Sci. Results,* 106/109: College Station, TX (Ocean Drilling Program), 263–267.

Böhlke, J. K., Honnorez, J., Honnorez-Guerstein, B. M., Muelenbachs, K., and Petersen, N., 1981. Heterogeneous alteration of the upper oceanic crust: correlation of rock chemistry, magnetic properties and O isotope ratios and alteration patterns in basalt from Site 396B, DSDP. *J. Geophys. Res.,* 86:7935–7950.

Burch, S. H., 1965. Tectonic emplacement of the Burro Mountain ultramafic body, southern Santa Lucia Range, California [Ph.D. dissert.]. Stanford Univ., Stanford, CA.

Coleman, R. G., 1971. Petrologic and geophysical nature of serpentinites. *Geol. Soc. Am. Bull.,* 82:897–918.

Collinson, D. W., 1983. *Methods in Rock Magnetism and Palaeomagnetism: Techniques and Instrumentation:* London (Chapman and Hall).

Day, R., Osterhoudt, M., and Bleil, U., 1983. Rock magnetism of igneous rocks from DSDP Sites 482, 483, and 485. *In* Lewis, B.T.R., Robinson, P., et al., *Init. Repts. DSDP,* 65: Washington (U.S. Govt. Printing Office), 727–736.

Dunlop, D. J., and Prevot, M., 1982. Magnetic properties and opaque mineralogy of drilled submarine intrusive rocks. *Geophys. J. R. Astron. Soc.,* 69:763–802.

Fox, P. J., and Opdyke, N. D., 1973. Geology of the oceanic crust: magnetic properties of oceanic rocks. *J. Geophys. Res.,* 78:5139–5154.

Fryer, P., Pearce, J. A., Stokking, L. B., et al., 1990. *Proc. ODP, Init. Repts.,* 125: College Station, TX (Ocean Drilling Program).

Fuller, M., Cisowski, S., Hart, M., Haston, R., Schmidtke, E., and Jarrard, R., 1988. NRM:IRM demagnetization plots: an aid to the interpretation of natural remanent magnetization. *Geophys. Res. Lett.,* 15:518–521.

Furuta, T., Tonouchi, S., and Nakada, M., 1980. Magnetic properties of pillow basalt from the Kinan Seamount chain, the Shikoku Basin. *J. Geomagn. Geoelectr.,* 32:567–573.

Gee, J., Tauxe, L., Hildebrand, J. A., Staudigel, H., and Lonsdale, P., 1988. Non-uniform magnetization of Jasper Seamount. *J. Geophys. Res.,* 93:12159–12175.

Griscom, A., 1964. Magnetic properties and aeromagnetic interpretation of serpentinite from southwest Puerto Rico. *In* Burk, C. A. (Ed.), *A Study of Serpentinite: the AMSOC Core Hole Near Mayagüez, Puerto Rico:* Natl. Acad. Sci., Natl. Res. Council, 1188:39–48.

Gromme, S., and Vine, F. J., 1972. Paleomagnetism of Midway Atoll lavas and northward movement of the Pacific plate. *Earth Planet. Sci. Lett.,* 17:159–168.

Hall, J. M., 1976. Major problems regarding the magnetization of oceanic crustal Layer 2. *J. Geophys. Res.,* 81:4223–4230.

Hamano, Y., Bina, M. M., and Krammer, K., 1990. Paleomagnetism of the serpentinized peridotite from ODP Hole 670A. *In* Detrick, R., Honnorez, J., Bryan, W. B., Juteau, T., et al., *Proc. ODP, Sci. Results,* 106/109: College Station, TX (Ocean Drilling Program), 257–262.

Hussong, D. M., and Fryer, P., 1981. Structure and tectonics of the Mariana arc and forearc: drilling site selection surveys. *In* Hussong, D. M., Uyeda, S., et al., *Init. Repts. DSDP,* 60: Washington (U.S. Govt. Printing Office), 33–44.

Kono, M., 1980. Paleomagnetism of DSDP Leg 55 basalts and implications for the tectonics of the Pacific plate. *In* Jackson, E. D., Koizumi, I., et al., *Init. Repts. DSDP,* 55: Washington (U.S. Govt. Printing Office), 737–752.

Krammer, K., 1990. Rock magnetic properties and opaque mineralogy of selected samples from Hole 670A. *In* Detrick, R., Honnorez, J., Bryan, W. B., Juteau, T., et al., *Proc. ODP, Sci. Results,* 106/109: College Station, TX (Ocean Drilling Program), 269–273.

Lienert, B. R., and Wasilewski, P. J., 1979. A magnetic study of the serpentinization process at Burro Mountain, California. *Earth Planet. Sci. Lett.,* 43:406–416.

Lowrie, W., and Fuller, M., 1971. On the alternating field demagnetization characteristics of multidomain thermoremanent magnetization of magnetite. *J. Geophys. Res.,* 76:6339–6349.

Lowrie, W., Løvlie, R., and Opdyke, N. D., 173a. Magnetic properties of DSDP basalts from the North Pacific Ocean. J. *Geophys. Res.,* 78:7647-7660.

———, 1973b. The magnetic properties of deep-sea drilling project basalts from the Atlantic Ocean. *Earth Planet. Sci. Lett.,* 17:338–349.

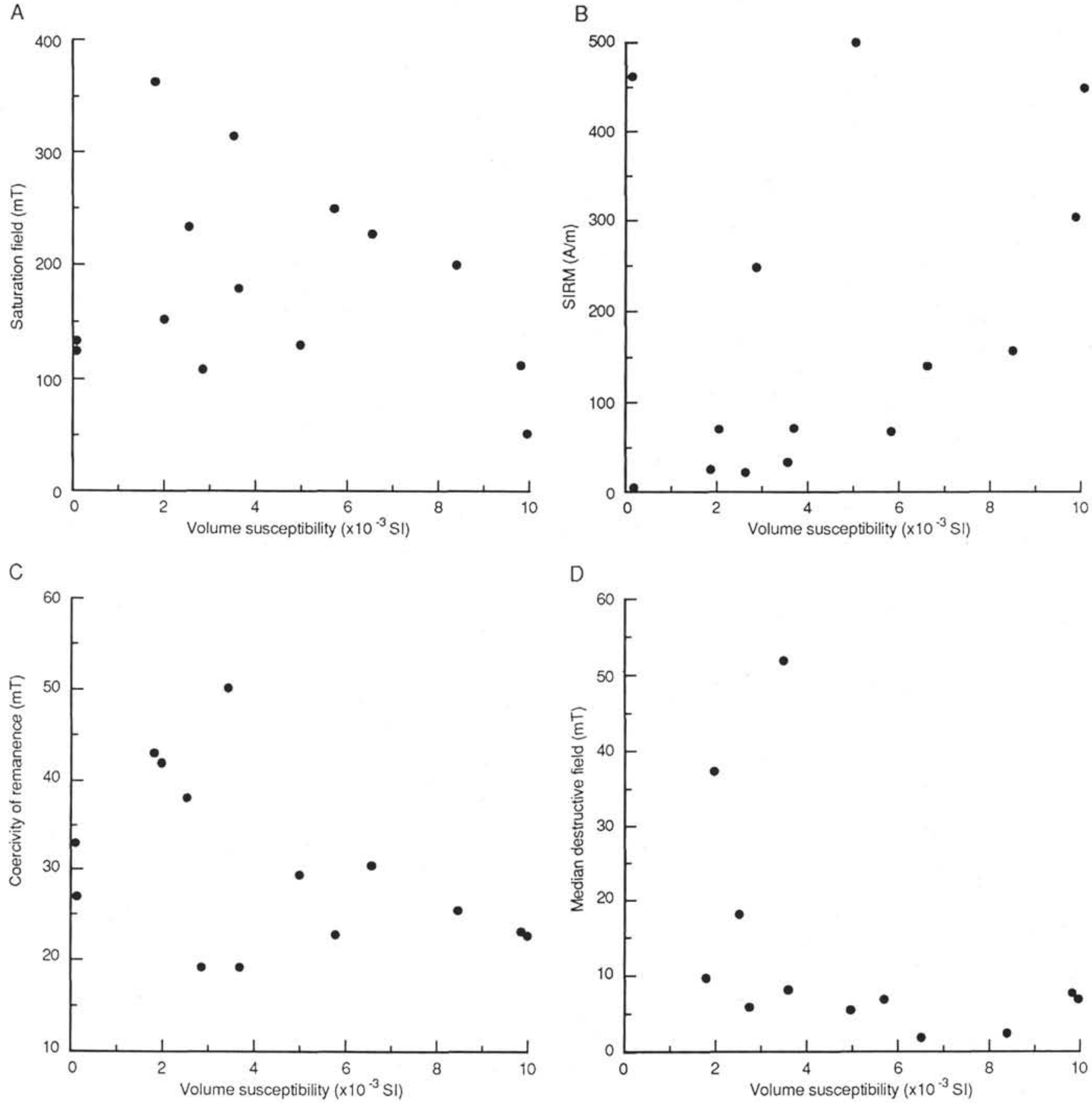


Figure 11. Volume susceptibility vs. rock magnetic properties (**A.** saturation field, **B.** SIRM intensity, **C.** coercivity of remanence, **D.** median destructive field), serpentinized peridotites, Leg 125.

Luyendyk, B. P., and Day, R., 1982. Paleomagnetism of the Samail ophiolite, Oman: 2. The Wadi Kadir gabbro section. *J. Geophys. Res.,* 87:10903–10917.

Luyendyk, B. P., Laws, B. R., Day, R., and Collinson, T. B., 1982. Paleomagnetism of the Samail ophiolite, Oman: 1. The sheeted dike complex at Ibra. *J. Geophys. Res.,* 87:10883–10902.

Marshall, M., 1978. The magnetic properties of some DSDP basalts from the North Pacific and inferences for Pacific plate tectonics. *J. Geophys. Res.,* 83:289–308.

Merrill, R. T., and Burns, R. E., 1972. A detailed magnetic study of Cobb Seamount. *Earth Planet. Sci. Lett.,* 14:413–418.

Merrill, R. T., and McElhinny, M. W., 1983. *The Earth's Magnetic Field: Its History, Origin, and Planetary Perspective:* London (Academic Press).

Pick, T., and Tauxe, L., 1991. CRM in synthetic magnetite. *J. Geophys. Res.,* 96:9925–9936.

Rice, P. D., Hall, J. M., and Opdyke, N. D., 1980. A paleomagnetic study of the Bermuda Seamount. *Can. J. Earth Sci.,* 17:232–243.

Saad, A. H., 1969a. Magnetic properties of ultramafic rocks taken from Red Mountain, CA. *Geophysics,* 34:974–987.

————, 1969b. Paleomagnetism of Franciscan ultramafic rocks from Red Mountain, California. *J. Geophys. Res.,* 74:6567–6578.

Shive, P. N., Frost, B. R., and Peretti, A., 1988. The magnetic properties of metaperidotitic rocks as a function of metamorphic grade: implications for crustal magnetic anomalies. *J. Geophys. Res.*, 93:12187–12195.
Silver, E. A., 1969. Late Cenozoic underthrusting of the continental margin off northernmost California. *Science*, 166:1265–1266.
Smith, G. M., 1985. Source of marine magnetic anomalies: some results from DSDP Leg 83. *Geology*, 13:162–165.
Stacey, F. D., and Banerjee, S. K., 1974. *Developments in Solid Earth Geophysics* (Vol. 5): *The Physical Principles of Rock Magnetism:* Elsevier (New York).
Stokking, L. B., and Tauxe, L., 1990. Properties of chemical remanence in synthetic hematite: testing theoretical predictions. *J. Geophys. Res.*, 95:12639–12652.
Swift, B. A., and Johnson, H. P., 1984. Magnetic properties of the Bay of Islands ophiolite suite and implications for the magnetization of oceanic crust. *J. Geophys. Res.*, 89:3291–3308.
Van Wagoner, N. A., and Johnson, H. P., 1983. Magnetic properties of three segments of the Mid-Atlantic Ridge at 37°N: FAMOUS, Narrowgate and AMAR:AMAR 2. *J. Geophys. Res.*, 88:5065–5082.

**Date of initial receipt: 1 October 1990**
**Date of acceptance: 6 May 1991**
**Ms 125B-158**

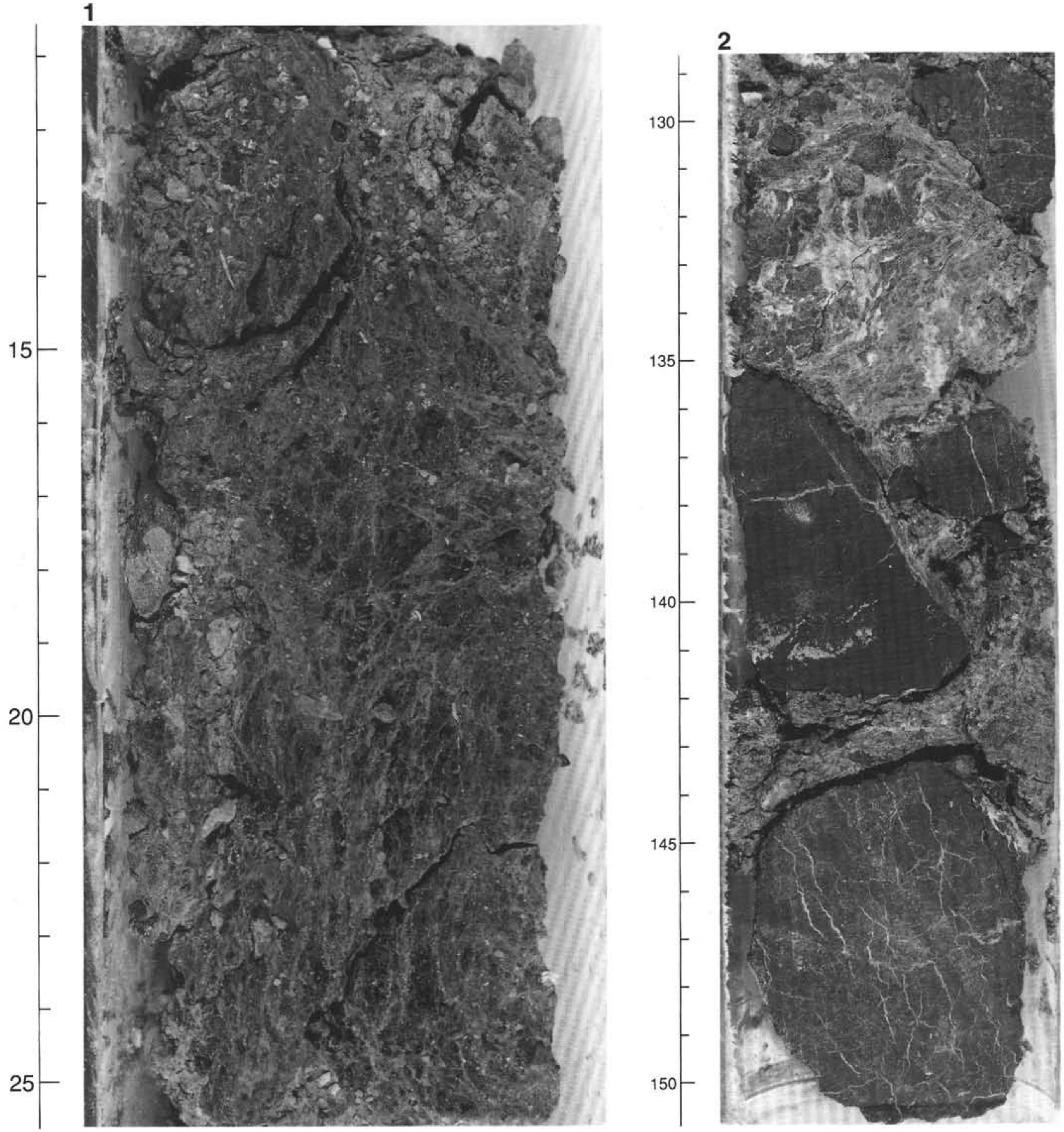


Plate 1. Core photographs illustrating representative rocks from Leg 125. **1.** Sheared phacoidal serpentine (Section 125-778A-11R-1, 11–25 cm). **2.** Sheared phacoidal serpentine containing clasts of serpentinized harzburgite (Section 125-784A-38R-1, 130–150 cm). **3.** Serpentinized dunite cut by two generations of veins (Section 125-779A-17R-2, 10–23 cm). The wide (2 cm) vein contains dark gray-green serpentine and magnetite that is cut by veins of chrysotile.

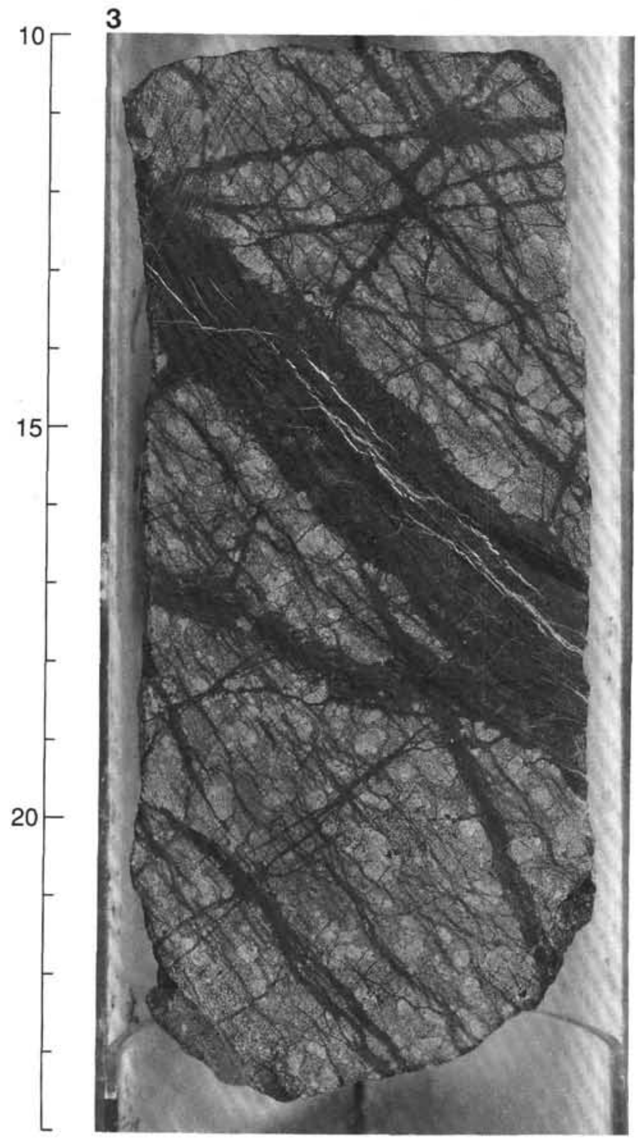


Plate 1 (continued).

1

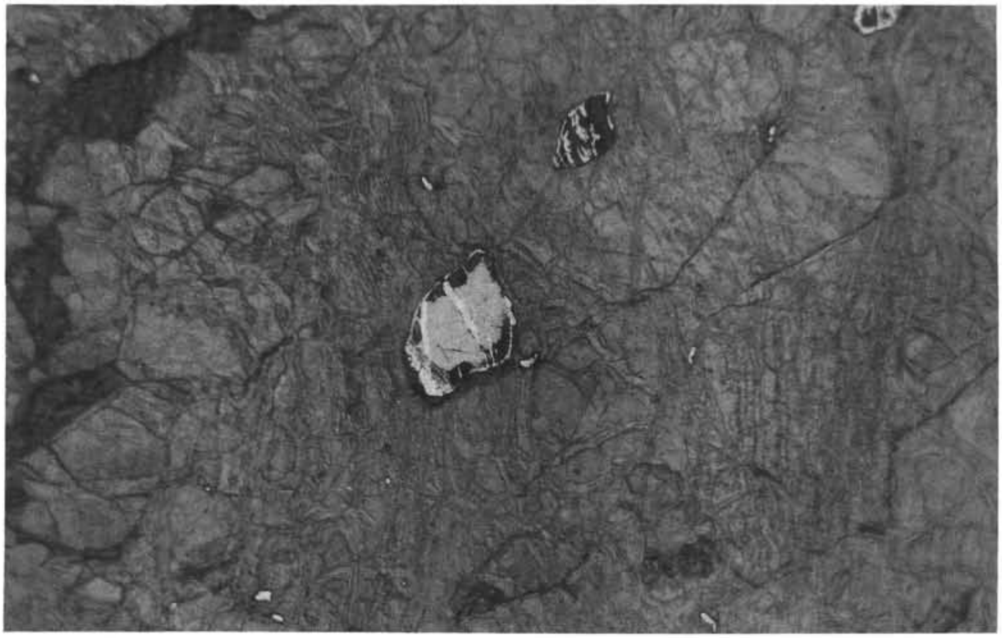

2

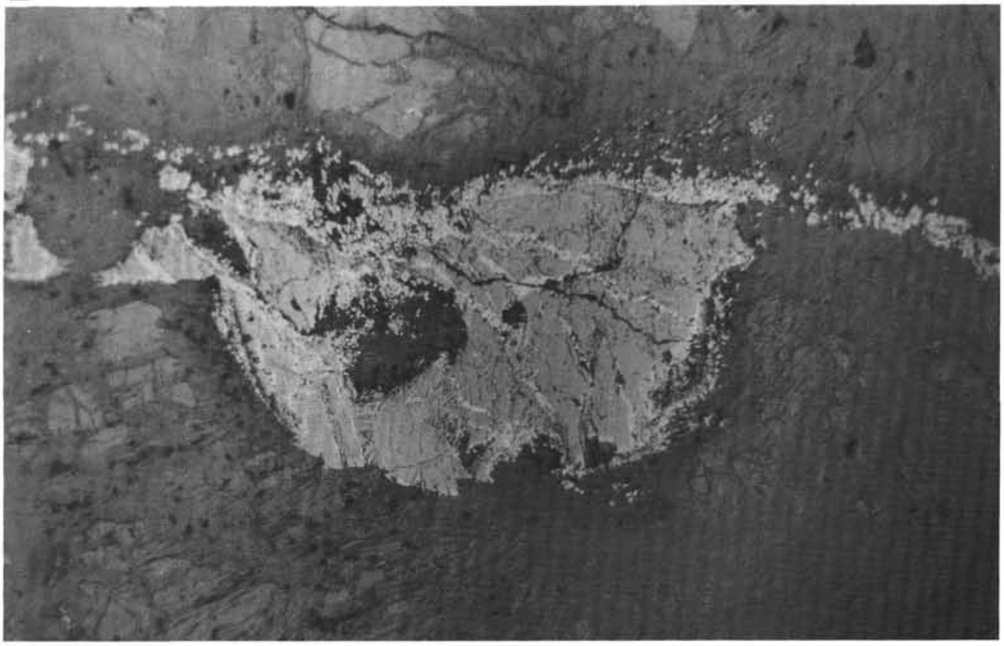

Plate 2. Photomicrographs illustrating the modes of occurrence of serpentinized peridotites from Leg 125. Scale bar is 100 µm. **1.** Reflected-light photomicrograph of Sample 125-778A-9R-1, 9–11 cm, a serpentinized harzburgite. The large grain in the center of the photograph is chromium-spinel that contains veins and a rim of magnetite (brighter material). **2.** Reflected-light photomicrograph of Sample 125-780C-13R-1, 56–59 cm, a serpentinized harzburgite. The central part of the photomicrograph is a chromium-spinel grain that is being replaced by magnetite (brighter material). The magnetite also occurs in association with serpentine in a vein adjacent to the chromium-spinel. **3.** Reflected-light photomicrograph of Sample 125-780C-13R-1, 56–59 cm, a serpentinized harzburgite. Magnetite particles (brighter material) line cleavage planes of an orthopyroxene grain (opx) and form elongate stringers in a vein that also contains serpentine. 4. Reflected-light photomicrograph of Sample 125-778A-9R-1, 9–11 cm, a serpentinized harzburgite. Magnetite particles (elongate stringers of brighter material) form veins, also containing serpentine, that outline less altered portions of the rock. Magnetite replaces chromium-spinel in the upper right corner.

3

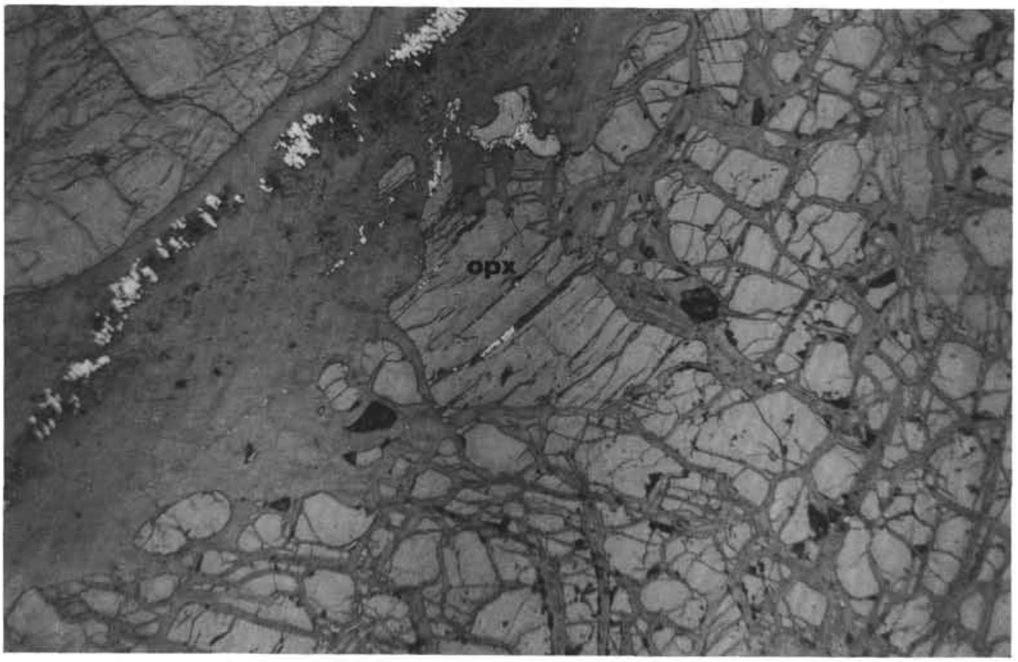


4

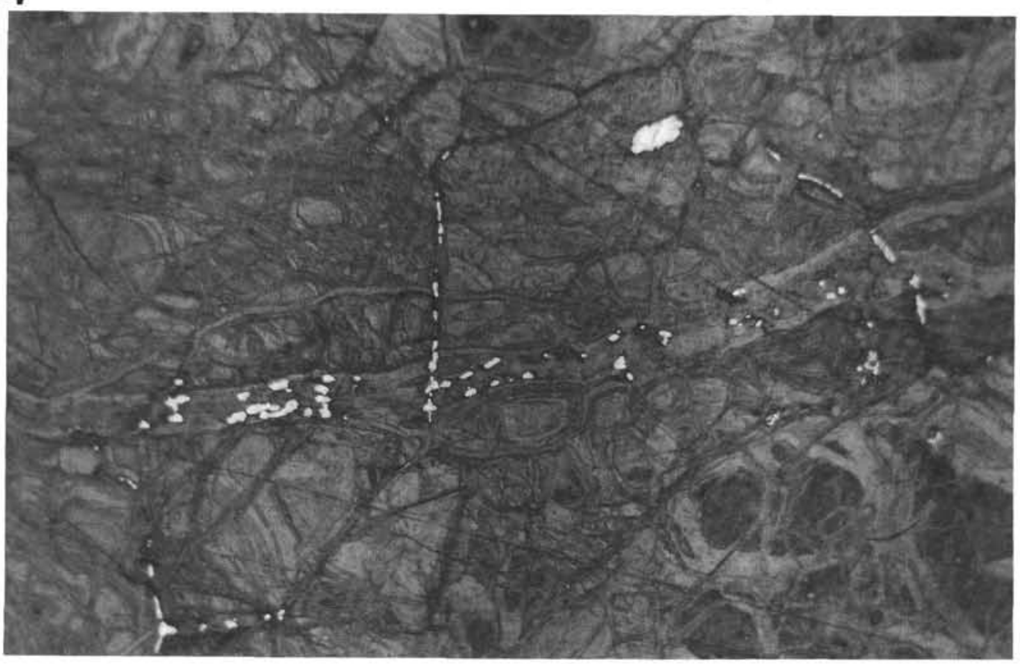

Plate 2 (continued).